Theory of High T_c Ferrimagnetism in a Multiorbital Mott Insulator

O. Nganba Meetei,[1] Onur Erten,[1] Mohit Randeria,[1] Nandini Trivedi,[1] and Patrick Woodward[2]

[1]*Department of Physics, The Ohio State University, Columbus, Ohio 43210, USA*
[2]*Department of Chemistry, The Ohio State University, Columbus, Ohio 43210, USA*

We propose a model for the multiorbital material Sr_2CrOsO_6, an insulator with remarkable magnetic properties and the highest $T_c \simeq 725$ K among *all* perovskites with a net moment. We derive a new criterion for the Mott transition $(\tilde{U}_1 \tilde{U}_2)^{1/2} > 2.5W$ by using slave-rotor mean field theory, where W is the bandwidth and $\tilde{U}_{1(2)}$ are the effective Coulomb interactions on Cr(Os) including Hund's coupling. We show that Sr_2CrOsO_6 is a Mott insulator, where the large Cr $\tilde{U}_1$ compensates for the small Os $\tilde{U}_2$. The spin sector is described by a frustrated antiferromagnetic Heisenberg model that naturally explains the net moment arising from canting and also the observed nonmonotonic magnetization $M(T)$. We predict characteristic magnetic structure factor peaks that can be probed by neutron experiments.

Transition metal oxides [1] with partially filled 3*d* and 4*d* shells have dominated materials research in past decades, leading to such spectacular phenomena as high T_c superconductivity and colossal magnetoresistance. We expect the next revolution to involve 5*d* oxides where the interplay of spin-orbit coupling (SOC) and strong correlations can lead to novel phases of matter. Recent experimental efforts have focused on iridium oxides [2–5], driven by the possibility of exotic phases [6–9]. Here we explore other equally promising experimental systems, the 5*d* oxides containing osmium that have received far less attention and provide a rich area for investigation.

We focus on the double perovskite (DP) family of oxides with the formula $A_2BB'O_6$. A is an alkali or alkaline earth metal, while B and B' are two transition metals arranged on a 3D checkerboard lattice. With two transition metal ions, the range of properties span metals to insulators, ranging from ferromagnets, antiferromagnets, ferroelectrics, and multiferroics to spin liquids [10–13].

The most studied DP is Sr_2FeMoO_6, a half-metallic ferrimagnet with $T_c \approx 420$ K [11,14]. It is now understood that a generalized double exchange mechanism can explain ferromagnetism with the scale of T_c set by the kinetic energy of itinerant electrons [15]. From this perspective, the observation of an even higher $T_c \approx 725$ K, the highest T_c among *all* perovskites with a net moment, in an insulator Sr_2CrOsO_6 (SCOO) [16] is rather puzzling.

There have been several important density functional theory (DFT) calculations of SCOO [16–19]; nevertheless, many puzzling questions remain open. (i) Why is SCOO an insulator [20]? It is not a band insulator, since the bands are partially filled. It is not obviously a Slater insulator, given the large moment observed on Cr. It is not *a priori* clear how it can be a Mott insulator either, given the weak correlations on Os relative to the large bandwidth of 5*d* orbitals. (ii) Why is there a net moment, given that both Cr and Os are in d^3 configurations? What is the role of

SOC on Os? DFT calculations [17,19] find a net moment only if SOC is included, but x-ray magnetic circular dichroism (XMCD) experiments [16] show insignificant Os orbital moment. (iii) What sets the scale for the high magnetic $T_c \simeq 725$ K? DFT does not give a clear answer [21]. (iv) Why is the magnetization $M(T)$ a nonmonotonic function [16] of T? Finite temperature properties are, of course, very hard for DFT to address.

In this Letter, we gain insight into all these questions within a theoretical framework that describes the hierarchy of energy scales in the charge and spin sectors. (1) We use a slave-rotor mean field theory to analyze the charge sector of SCOO and show that it is a multiorbital Mott insulator. We derive a new criterion for the Mott transition for this system: $(\tilde{U}_1 \tilde{U}_2)^{1/2} > 2.5W$, where W is the bandwidth and $\tilde{U}_{1(2)}$ the effective Coulomb repulsion on Cr(Os), which includes the important effects of Hund's coupling in addition to Hubbard U. Thus a small $\tilde{U}_2$ on Os is compensated by a strong $\tilde{U}_1$ on Cr and drives the system into a Mott insulating state. (2) We find that the orbital angular momentum on Os is quenched, and the Os moment is purely of spin origin, in agreement with XMCD measurements [16]. (3) We show that the effective spin Hamiltonian for SCOO is a frustrated Heisenberg model with antiferromagnetic exchange between nearest neighbor Cr-Os as well as next-nearest neighbor Os-Os spins. We find that the net magnetic moment $M(0)$ arises, not because of SOC, but rather because of a canted magnetic ground state, found by using both Monte Carlo (MC) simulations and a variational approach. (4) The scale for the high T_c is set by a $J_1 = 35$ meV superexchange between Cr-Os near neighbors. (5) We find that we can obtain an unusual nonmonotonic $M(T)$, in agreement with magnetization and neutron experiments [16], due to a subtle frustration effect between Cr-Os J_1 and Os-Os J_2. (6) Finally, we predict distinct magnetic structure factor peaks for our canted ground state. These can be measured by neutrons and provide a "smoking gun" test of our theory.

Hamiltonian.—The cubic crystal field splits d orbitals and only the t_{2g} orbitals are occupied, with both Cr and Os in d^3 configurations. To investigate the metal-insulator transition, we consider

$$H = -t \sum_{\langle ij \rangle, \alpha} (d_{i\alpha}^\dagger c_{j\alpha} + \text{H.c.}) - t' \sum_{\langle\langle ij \rangle\rangle, \alpha} (c_{i\alpha}^\dagger c_{j\alpha} + \text{H.c.})$$
$$+ \frac{\tilde{U}_1}{2} \sum_i \left[\sum_\alpha n_{1i\alpha} \right]^2 + \frac{\tilde{U}_2}{2} \sum_i \left[\sum_\alpha n_{2i\alpha} \right]^2$$
$$- \mu \sum_{i,\alpha} (n_{1i\alpha} + n_{2i\alpha}) - \Delta \sum_{i,\alpha} (n_{1i\alpha} - n_{2i\alpha}). \quad (1)$$

This has orbitally symmetric on-site Coulomb interactions that make the problem analytically tractable and provide insight, while capturing the essence of strong correlations in a multiband system. Hund's coupling will be discussed below. Here $d_{i\alpha}^\dagger$ ($d_{i\alpha}$) and $c_{i\alpha}^\dagger$ ($c_{i\alpha}$) are the creation (annihilation) operators on the ith Cr and Os sites, respectively. $n_{1i\alpha}$ ($n_{2i\alpha}$) are the number operators on the ith Cr (Os) site. Note that the label α includes both spin and t_{2g} orbital index. t and t' are the hopping amplitude between neighboring Cr-Os and Os-Os sites. The effective on-site Coulomb interaction $\tilde{U}_{1(2)}$ is related to the atomic charge gap on Cr(Os), as discussed in detail below. The chemical potential is μ, and Δ is the charge transfer gap between Cr and Os.

Multiband Mott criterion.—We investigate the charge sector of (1) using the slave-rotor mean field (MF) theory [22]. This method captures the qualitative physics of dynamical mean field theory and is well suited to studying the multiband Mott transition; it has recently been used for various other multiband system including pyroclores and iron pnictides [8,23,24]. We decompose the physical electron into an O(2) rotor that carries the charge and a spinon that carries the spin and orbital degrees of freedom. We write $d_{i\alpha}^\dagger = f_{i\alpha}^\dagger e^{i\theta_i}$ and $c_{i\alpha}^\dagger = g_{i\alpha}^\dagger e^{i\phi_i}$, where $f_i^\dagger$ (f_i) and $g_i^\dagger$ (g_i) are the fermonic spinon creation (annihilation) operators on the ith Cr and Os sites, respectively. The bosonic rotor operator $\theta_i(\phi_i)$ is conjugate to the charge on Cr(Os) at site i. Substituting into (1) and performing a MF decomposition of the hopping terms, we obtain spinon and rotor Hamiltonians that we solve self-consistently.

We calculate $\langle\cos\theta\rangle$ and $\langle\cos\phi\rangle$, which are used as diagnostics of the metal-insulator transition. When both quantities vanish, the system is a Mott insulator with suppressed charge fluctuations, while nonzero values lead to a metal. For simplicity, we first work at the particle-hole (p-h) symmetric point: $\mu \equiv \mu_0 = 3(\tilde{U}_1 + \tilde{U}_2)/2$, $\Delta \equiv \Delta_0 = 3(\tilde{U}_1 - \tilde{U}_2)/2$, and $t' = 0$, where we can obtain analytical results [25]. We find

$$(\tilde{U}_1 \tilde{U}_2)^{1/2} > 2.5W, \quad (2)$$

where $W = 8t$ is the t_{2g} bandwidth. This new Mott criterion generalizes the well-known result $U \gtrsim W$.

Deviations from the p-h symmetric point, relevant for real materials, require numerical solution of the slave-rotor mean field equations. In general, the right-hand side of (2) is replaced by the the average kinetic energy, which depends on the filling and band structure [25].

The resulting phase diagram is shown in Fig. 1. We see from Fig. 1(c) that increasing t' favors the metallicity by introducing an additional route for gaining kinetic energy. Figure 1(d) shows that increasing the deviation from the symmetric point $\tilde{\Delta} \equiv \Delta - \Delta_0$, for a fixed $\mu = \mu_0$ and $t' = 0$, also favors metallicity, as it increases charge fluctuations within a unit cell [25].

Determining the effective U.—In order to apply our results to SCOO, we must relate the effective interaction $\tilde{U}_{1(2)}$ to material parameters: the Hubbard U, Hund's coupling J_H, and SOC ξ. This is done by matching the excitation energy in the atomic limit of (1) to that of the more general atomic Hamiltonian

$$H_a^{at} = (U_a - 3J_{Ha}) \frac{\hat{N}_a(\hat{N}_a - 1)}{2} - 2J_{Ha}(\mathbf{S}_a)^2$$
$$+ \frac{1}{2} J_{Ha}(\mathbf{T}_a)^2 - \lambda_a \mathbf{T}_a \cdot \mathbf{S}_a - \mu_a \hat{N}_a. \quad (3)$$

Here the label $a = 1, 2$ indicates Cr and Os sites, respectively. $\hat{N}$ is the total number operator, $\mathbf{S}$ the total spin operator, and $\mathbf{T}$ the total orbital angular momentum operator in the t_{2g} manifold. The effective SOC λ in a given TS
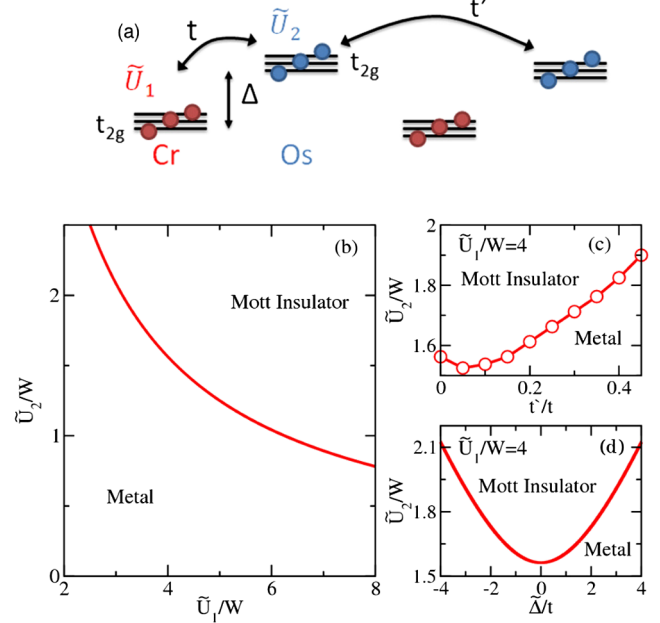

FIG. 1 (color online). Phase diagram obtained from slave-rotor mean field theory. (a) Schematic of Cr and Os orbitals and relevant energies. (b) Phase boundary of Eq. (2) for the particle-hole symmetric case $t' = 0$, $\Delta = \Delta_0$, and $\mu = \mu_0$; see the text. Combination of small $\tilde{U}_2$ on Os and large $\tilde{U}_1$ on Cr can drive the system Mott insulating. Effect of (c) Os-Os hopping t' and (d) Cr-Os charge-transfer energy Δ.

manifold is a function of T, S, and ξ [25]. We work with a d^3 atomic ground state.

For the Cr site, we ignore SOC and find the atomic excitation gap to obtain $\tilde{U}_1 = U_1 + 2J_{H1}$ [25]. The effective repulsion is enhanced by Hund's coupling, well known [26,27] for half filled orbitals. On the Os site, we include λ_2 and find $\tilde{U}_2 = U_2 + 2J_{H2} - 3\xi_2/2$ [25], so that SOC reduces the atomic charge gap.

We now can use our Mott criterion for SCOO. For Cr, we use $U_1 \approx 5$ eV and $J_{H1} \approx 1$ eV [1]. For Os, we use $U_2 \approx 2$ eV, $J_{H2} \approx 0.35$ eV, and $\xi_2 \approx 0.3$ eV [28]. Thus $(\tilde{U}_1 \tilde{U}_2)^{1/2} \approx 4$ eV, which is larger than the critical value $2.5W \approx 3.75$ eV using the band theory estimate $W \approx 1.5$ eV [19]. We thus believe that SCOO is a Mott insulator. We emphasize that (2) is a conservative criterion for a Mott insulator for two reasons. First, MF theory overestimates the stability of the metallic phase (which has long range order in the rotor sector). Second, the slave-rotor approach neglects magnetic order, which would further help charge localization.

It is worthwhile to check Eq. (2) for a ternary perovskite NaOsO$_3$, where it reduces to $\tilde{U} > 2.5W$. NaOsO$_3$ does not satisfy this inequality and is thus on the metallic side of the transition. This is in agreement with experiments [29,30] that show metallic behavior in the paramagnetic state, with spin density wave magnetism at low T. On the other hand, for a DP like SCOO, *it is the geometric mean of $\tilde{U}_1$ and $\tilde{U}_2$ that determines the effective strength of correlation*. Thus the small on-site $\tilde{U}_2$ on the $5d$ site Os is compensated by the large $\tilde{U}_1$ on the $3d$ site like Cr to drive the system Mott insulating.

Effective spin Hamiltonian.—Having shown that charge is localized, we turn to the spin sector. For simplicity, we take a strong coupling approach, although in reality SCOO is likely an intermediate coupling material (see concluding section). Given the large J_H on Cr, the three spins align to yield $S = 3/2$. We might expect that a large SOC $\lambda \mathbf{l} \cdot \mathbf{S}$ on Os might split the $5d$ t_{2g} orbitals into $J = 3/2$ and $J = 1/2$ manifolds. However, in the special case of a d^3 configuration, the orbital angular momentum is quenched. Thus we also get an $S = 3/2$ spin on Os. While the absence of an orbital moment on Os is consistent with XMCD data [16], we must now explain the net moment, since SOC cannot be responsible for this.

The effective spin Hamiltonian is given by

$$H_{\text{eff}} = J_1 \sum_{\langle ij \rangle} \mathbf{S}_i^1 \cdot \mathbf{S}_j^2 + J_2 \sum_{\langle\langle ij \rangle\rangle} \mathbf{S}_i^2 \cdot \mathbf{S}_j^2. \quad (4)$$

Here $\mathbf{S}_i^{1(2)}$ is a classical $S = 3/2$ spin on the ith Cr(Os) site; see Fig. 2(b). Given the general rules of superexchange for half filled orbitals, J_1 between Cr-Os and J_2 between Os-Os are both antiferromagnetic. We have retained next-nearest neighbor Os-Os couplings, because $5d$ orbitals are much more extended than $3d$ orbitals. J_1 tends to order the spins into a Néel antiferromagnet, while J_2 frustrates this ordering. Note that J_2 by itself is also frustrated, since Os
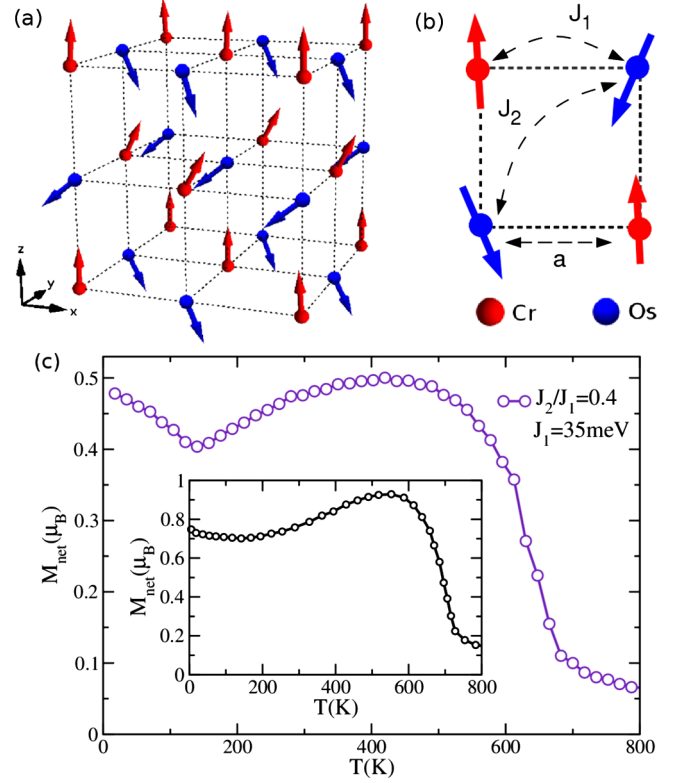

FIG. 2 (color online).   (a) Canted ground state obtained from MC simulations (4096 spins, $J_2/J_1 = 0.4$). (b) Schematic showing the antiferromagnetic interactions. (c) $M(T)$ for $J_2/J_1 = 0.4$. By comparing with experimental T_c we obtain $J_1 = 35$ meV. Note that $M(T = 0)$ is finite and $M(T)$ has an unusual non-monotonic behavior in agreement with experimental data in the inset [16].

spins are on an fcc lattice. Given the complexity of estimating superexchange microscopically [31], we treat them as parameters and study the magnetic properties as a function of J_2/J_1.

Magnetic structure.—In Fig. 2(a), we show the magnetic ground state obtained from MC simulation of H_{eff} for $J_2/J_1 = 0.4$. The magnetic structure factor has two large peaks at $\mathbf{q}_0 = (\pi, \pi, \pi)/a$ and $\mathbf{q}_1 = (\pi, \pi, 0)/a$, where a is the nearest neighbor Cr-Os separation. We gain insight into this ground state by using a variational analysis. Fourier transforming (4), we get $H_{\text{eff}} = \sum_q \boldsymbol{\psi}^\dagger(\mathbf{q}) \cdot H(\mathbf{q}) \cdot \boldsymbol{\psi}(\mathbf{q})$, where $H_{11} = 0$, $H_{12} = H_{21} = J_1[\cos(q_x a) + \cos(q_y a) + \cos(q_z a)]$, $H_{22} = J_2\{\cos[(q_x - q_y)a] + \cos[(q_y - q_z)a] + \cos[(q_x - q_z)a]\}$ and $\boldsymbol{\psi}^\dagger = [\mathbf{S}^1(\mathbf{q})^*, \mathbf{S}^2(\mathbf{q})^*]$. For each $\mathbf{q}$ we diagonalize $H(\mathbf{q})$ and find that $\mathbf{q}_0 = (\pi, \pi, \pi)/a$, the usual antiferromagnetic Néel ordering of Cr and Os spins, minimizes the energy. While it satisfies $|\mathbf{S}_i^1|^2 + |\mathbf{S}_i^2|^2 = 2S^2$, it does not satisfy the constraints $|\mathbf{S}_i^1|^2 = S^2$ and $|\mathbf{S}_i^2|^2 = S^2$ for $J_2/J_1 \neq 0$.

Upon generalizing the solution to include two different $\mathbf{q}$'s that minimize the energy and also satisfy the constraints, we find that $\mathbf{q}_0 = (\pi, \pi, \pi)/a$ and

$\mathbf{q}_1 = (\pi, \pi, 0)/a$ in agreement with the MC results. Our prediction of the structure factor peaks can be checked by neutron scattering and should prove to be an important test of our theory.

Magnetization $M(T)$.—We calculate $M(T)$ in 3D by using finite temperature classical MC simulations. Figure 2(c) shows that (i) $M(T = 0)$ is finite, (ii) $M(T)$ has an unusual nonmonotonic function of temperature, and (iii) a large value of T_c for $J_1 = 35$ meV and $J_2/J_1 = 0.4$. Remarkably, all of these results compare very well with experimental data shown in the inset in Fig. 2(c) [16].

The nonzero value of $M(0)$ arises from the canted nature of the ground state discussed above; see Fig. 2(a). There are some quantitative differences with experiment, e.g., $M(T = 0) \approx 0.75\mu_B$ and it peaks at $\approx 0.9\mu_B$ while the simulation gives $M(T = 0) \approx 0.5\mu_B$, which could be due to any one of several effects ignored in our minimal model, like higher order effects of SOC or distortion from the cubic lattice.

The nonmonotonicity of the net $M(T)$ arises from a competition between the magnetizations on the two sublattices: for essentially antiparallel moments $M = M_{Cr} - M_{Os}$. At low T, the Os moments are stuck in the canted state, and M_{Os} does not change significantly with temperature. However, M_{Cr} drops faster, leading to a decrease in M. This trend continues till about 150 K. At intermediate temperatures, Os spins have a smaller spin stiffness compared to Cr spins, because J_2 acts only on the Os sublattice. Thus Os spins become more "floppy" and depolarize faster, leading to an increase in M with temperature. Close to T_c both Cr and Os moments drop very rapidly, and the net moment goes to zero at T_c. This provides a qualitative understanding of the nonmonotonic behavior. The behavior shown in Fig. 2(c) depends sensitively on the choice of J_2/J_1 and $M(T)$ for different J_2/J_1 is discussed in Ref. [25].

Discussion.—For weakly correlated materials, the magnetism is of the Slater or spin-density wave form where the state above T_c is a metal and the charge gap is determined by magnetic ordering, In a local-moment Mott insulator, the charge gap scale is set by the Coulomb interaction and is much larger than T_c, set by superexchange. SCOO is in effect just on the Mott side of this crossover between Slater and Mott magnetism. By combining a weakly interacting $5d$ Os with a strongly interacting $3d$ Cr, we are able to tune the interaction strength to an intermediate regime and, therefore, maximize the T_c. We already see some evidence for the emergence of such a crossover behavior: NaOsO$_3$ is a Slater insulator with a $T_N \approx 410$ K, while LaCrO$_3$ a strong coupling Mott insulator with a 3.5 eV charge gap and $T_N \approx 320$ K. SCOO is at an intermediate coupling on the Mott side, and this generates a very high ordering temperature.

Moreover, the insulating and magnetic mechanisms that we have unravelled in SCOO are an important step for

TABLE I. Oxides of Cr and Os, where I denotes insulators, M metals, AF antiferromagnets, and Fi ferrimagnets. The Weiss constant θ is not available for materials with high T_c.

Sc	Ti	V	Cr	Mn	Fe	Co
			Mo	Tc	Ru	Rh
			W	Re	Os	Ir

		T_c (K)	θ (K)		Ref.
Sr$_2$ScOsO$_6$	I AF	25	-636	Sc^{3+}($3d^0$) Os^{5+}($5d^3$)	[32]
Sr$_2$CrOsO$_6$	I Fi	725	$\ldots$	Cr^{3+}($3d^3$) Os^{5+}(d^3)	[16]
Sr$_2$FeOsO$_6$	I Fi	65	$+37$	Fe^{3+}($3d^5$) Os^{5+}($5d^3$)	[33]
Sr$_2$CoOsO$_6$	I Fi	65, 110	$\ldots$	Fe^{2+}($3d^7$) Os^{6+}($5d^2$)	[33]
Sr$_2$CrWO$_6$	M Fi	458	$\ldots$	Cr^{3+}($3d^3$) W^{5+}($5d^1$)	[34]
Sr$_2$CrReO$_6$	? Fi	635	$\ldots$	Cr^{3+}($3d^3$) Re^{5+}($5d^2$)	[35,36]
NaOsO$_3$	I AF	410	$\ldots$	Os^{5+}($5d^3$)	[29,30]
LaCrO$_3$	I AF	320	-750	Cr^{3+}($3d^3$)	[37,38]

understanding the trends, such as metal to insulator transitions, in materials with fixed Os and varying $3d$ ion (Sc-Cr-Fe-Co), as well as fixed Cr and varying $5d$ ion (W-Re-Os) [see Table I].

Conclusion.—We have established a general theoretical framework for understanding Mott insulators in DPs with half filled bands. It can be easily generalized to other materials like Sr$_2$MnOsO$_6$ and Sr$_2$FeOsO$_6$ [39]. An important open question is the effect of doping these multiband Mott insulators. Away from half filling, SOC will become important, and the interplay of strong SOC and interactions may produce exciting new physics.

[1] M. Imada, A. Fujimori, and Y. Tokura, Rev. Mod. Phys. **70**, 1039 (1998).
[2] B. J. Kim, H. Ohsumi, T. Komesu, S. Sakai, T. Morita, H. Takagi, and T. Arima, Science **323**, 1329 (2009).
[3] X. Liu, T. Berlijn, W.-G. Yin, W. Ku, A. Tsvelik, Y.-J. Kim, H. Gretarsson, Y. Singh, P. Gegenwart, and J. P. Hill, Phys. Rev. B **83**, 220403 (2011).
[4] K. Matsuhira, M. Wakeshima, R. Nakanishi, T. Yamada, A. Nakamura, W. Kawano, S. Takagi, and Y. Hinatsu, J. Phys. Soc. Jpn. **76**, 043706 (2007).
[5] Y. Okamoto, M. Nohara, H. Aruga-Katori, and H. Takagi, Phys. Rev. Lett. **99**, 137207 (2007).
[6] G. Jackeli and G. Khaliullin, Phys. Rev. Lett. **102**, 017205 (2009).
[7] X. Wan, A. M. Turner, A. Vishwanath, and S. Y. Savrasov, Phys. Rev. B **83**, 205101 (2011).
[8] D. Pesin and L. Balents, Nat. Phys. **6**, 376 (2010).

[9] F. Wang and T. Senthil, Phys. Rev. Lett. **106**, 136402 (2011).

[10] D. Serrate, J. M. D. Teresa, and M. R. Ibarra, J. Phys. Condens. Matter **19**, 023201 (2007).

[11] K.-I. Kobayashi, T. Kimura, H. Sawada, K. Terakura, and Y. Tokura, Nature (London) **395**, 677 (1998).

[12] G. Chen, R. Pereira, and L. Balents, Phys. Rev. B **82**, 174440 (2010).

[13] G. Chen and L. Balents, Phys. Rev. B **84**, 094420 (2011).

[14] D. D. Sarma, P. Mahadevan, T. Saha-Dasgupta, S. Ray, and A. Kumar, Phys. Rev. Lett. **85**, 2549 (2000).

[15] O. Erten, O. N. Meetei, A. Mukherjee, M. Randeria, N. Trivedi, and P. Woodward, Phys. Rev. Lett. **107**, 257201 (2011).

[16] Y. Krockenberger et al., Phys. Rev. B **75**, 020404 (2007).

[17] H. Das, P. Sanyal, T. Saha-Dasgupta, and D. D. Sarma, Phys. Rev. B **83**, 104418 (2011).

[18] T. K. Mandal, C. Felser, M. Greenblatt, and J. Kübler, Phys. Rev. B **78**, 134431 (2008).

[19] K.-W. Lee and W. E. Pickett, Phys. Rev. B **77**, 115101 (2008).

[20] DFT results for insulating behavior depend on approximation. Local spin density approximation with SOC yields a metal [19], LDA + U gives an insulator [19], and generalized gradient approximation [18] an insulator with a much larger gap than generalized gradient approximation with SOC [16,17].

[21] The only DFT calculation [18] that estimates T_c ignores SOC and yields an antiferromagnetic ground state with zero net moment and an order-of-magnitude larger gap compared with other DFT calculations [17,19].

[22] S. Florens and A. Georges, Phys. Rev. B **70**, 035114 (2004).

[23] W.-H. Ko and P. A. Lee, Phys. Rev. B **83**, 134515 (2011).

[24] M. Kargarian, J. Wen, and G. A. Fiete, Phys. Rev. B **83**, 165112 (2011).

[25] See Supplemental Material at http://link.aps.org/supplemental/10.1103/PhysRevLett.110.087203 for technical details of our calculations and additional information.

[26] J. E. Han, M. Jarrell, and D. L. Cox, Phys. Rev. B **58**, R4199 (1998).

[27] L. de' Medici, J. Mravlje, and A. Georges, Phys. Rev. Lett. **107**, 256401 (2011).

[28] K.-W. Lee and W. E. Pickett, Europhys. Lett. **80**, 37 008 (2007).

[29] S. Calder et al., Phys. Rev. Lett. **108**, 257209 (2012).

[30] Y. Shi et al., Phys. Rev. B **80**, 161104 (2009).

[31] P. Fazekas, Lecture Notes on Electron Correlation and Magnetism (World Scientific, Singapore, 1999).

[32] J.-H. Choy, D.-K. Kim, and J.-Y. Kim, Solid State Ionics **108**, 159 (1998).

[33] R. Morrow and P. Woodward (unpublished).

[34] J. B. Philipp et al., Phys. Rev. B **68**, 144431 (2003).

[35] H. Kato, T. Okuda, Y. Okimoto, Y. Tomioka, Y. Takenoya, A. Ohkubo, M. Kawasaki, and Y. Tokura, Appl. Phys. Lett. **81**, 328 (2002).

[36] A. J. Hauser et al., Phys. Rev. B **85**, 161201 (2012).

[37] W. C. Koehler and E. O. Wollen, J. Phys. Chem. Solids **2**, 100 (1957).

[38] K. Sardar, M. R. Lees, R. J. Kashtiban, J. Sloan, and R. I. Walton, Chem. Mater. **23**, 48 (2011).

[39] Substituting Cr with Mn(Fe) will change Δ and filling. Our theory can account for Δ, while the extra electrons will go to the e_g band. The large charge transfer gap between Os e_g and Mn(Fe) e_g levels leads to a narrow e_g band, which can be easily localized.